

See discussions, stats, and author profiles for this publication at: <https://www.researchgate.net/publication/231644432>

CO₂ Activation and Total Reduction on Titanium(0001) Surface

ARTICLE in THE JOURNAL OF PHYSICAL CHEMISTRY C · JUNE 2010

Impact Factor: 4.77 · DOI: 10.1021/jp100147g

CITATIONS

14

READS

25

2 AUTHORS:



Shunfang Li

Zhengzhou University

33 PUBLICATIONS 299 CITATIONS

SEE PROFILE



Z. Xiao Guo

University College London

201 PUBLICATIONS 3,959 CITATIONS

SEE PROFILE

CO₂ Activation and Total Reduction on Titanium(0001) Surface

S. F. Li^{†,‡} and Z. X. Guo^{*,†}

Department of Chemistry and London Centre for Nanotechnology, University College London, London WC1H 0AJ, U.K., and School of Physics and Engineering, Zhengzhou University, Zhengzhou 450052, P. R. China

Received: December 24, 2009; Revised Manuscript Received: May 23, 2010

From first-principles simulations, we identify that CO₂ is strongly activated and chemically adsorbed via both the carbon and the oxygen atoms and can totally dissociate on the Ti (0001) surface, under appropriate conditions, in contrast to relatively weak interactions of CO₂ with other transition metals reported previously. This strong activation is due to the relatively small work function or electronegativity of Ti. We postulate that a structure with a smaller work function provides greater activation for CO₂. The findings point to new directions for the design of efficient Ti-based alloy catalysts for CO₂ capture and conversion.

I. Introduction

Activation and reduction of carbon dioxide are of great significance in CO₂ sequestration and conversion, so as to mitigate climate change and utilize CO₂ as a resource. CO₂ activation is also an important step in many industrial processes, such as the methanol synthesis. Although CO₂ reduction occurs naturally in photosynthesis, resulting in the separation of carbon and oxygen, industrial conversion of CO₂ is very challenging due to the strong C=O bond. Some transition metals (TMs)¹ and metal–organic frameworks^{2,3} were considered to reduce CO₂ by multielectronic interactions to form organic materials, but the well-known catalytic TMs (and their oxides), such as Ru,⁴ Rh,⁵ Pd,⁶ Pt,⁷ Cu,⁸ Ag,⁹ and Fe,¹⁰ efficiently catalyze CO oxidization (CO + $\frac{1}{2}$ O₂ → CO₂), rather than CO₂ reduction, due to the high stability of CO₂ and their weak interactions.

Studies show that except for alkali-metal-promoted surfaces¹¹ and a few late TM elements, such as Fe,^{1b} Co,¹² Ni,¹³ and Cu,¹⁴ CO₂ adsorbs rather weakly on metal surfaces and is poorly activated. For example, CO₂ weakly bounds to a clean Pt(111)^{11a} with linear configuration and a large dissociation barrier of ~2.0 eV.^{11b} Recently, Glezakou et al.^{10c} identified that CO₂ can be activated by the Fe(100) surface with a bent structure and 16.7 kcal/mol binding energy. Freund et al.^{1b} report that CO₂ can be chemisorbed on the Fe(111) surface at high temperature, leading to a CO₂[−] state. However, the reduction of CO₂ is an endothermic process with a large activation barrier.^{1b,15} Very recently, Shea et al.¹² suggest that the Co(110) surface is likely to trigger CO₂ activation and hence facilitate CO₂ dissociation, and the adsorption energy reaches 0.606 eV when the C is at the short-bridge site. In fact, Ni(110)¹³ is claimed to be the only transition metal surface of low Miller indices to bind CO₂ chemically (0.32 eV) under ultrahigh vacuum without the coadsorption of alkali metals as electron donors,^{11a} where the CO₂ molecule prefers to “bend” slightly with evident charge transfer from the Ni substrate to the CO₂ moiety.¹³

Consequently, a challenging question arises: are there any other elements capable of strongly activating or reducing CO₂? Although several researchers report CO₂ interactions with metal surfaces,^{1,11–15} there is a paucity of reports on CO₂ reaction with the early TMs, such as Ti. However, we note that Azuma

et al.¹⁶ systematically investigated the electrochemical reduction of carbon dioxide on various metal electrodes in low-temperature aqueous KHCO₃ media and predicted that most of the light transition metals are not so effective for CO₂ reduction except for Ti. The key issues to be addressed are the following: How is the CO₂ molecule adsorbed on the Ti surface, and is it in dissociated or molecular form? Can we design Ti-based catalysts to heterogeneously activate CO₂? What is the underlying mechanism of the heterogeneous catalysis of Ti for CO₂ reduction?

In this paper, by means of first-principles simulations, we discovered that the Ti(0001) surface may not only activate but also reduce CO₂ into CO and O and can further completely dissociate the CO moiety into C and O in appropriate conditions, which can be explained by a charge transfer mechanism. Our results also simultaneously support a recent experimental finding that C can be introduced into TiO₂ by thermally pyrolyzing a Ti metal sheet in the presence of CO₂ and steam, resulting in a photocatalytic material of TiO_{2–x}C_x.¹⁷ Hence, it is expected that Ti may be used to alloy with other less reactive transition metals as an effective catalyst for CO₂ capture and conversion.

II. Methods

Our spin-polarized calculations were carried out using the Vienna *ab initio* simulation package (VASP)¹⁸ with the exchange–correlation energy corrections described by the Perdew–Burke–Ernzerhof¹⁹ parametrization. The interaction between the ions and valence electrons is described by the PAW potential²⁰ with an energy cutoff of 400 eV for the plane wave basis. We construct a five layer p(3 × 3) metal slab with a vacuum thickness of about 12 Å to model the Ti(0001) surface (the calculated lattice parameters are $a = 2.91$ Å and $c = 4.65$ Å, in close agreement with experimental values^{21a} and previously calculated results^{21b}). The two topmost surface layers and the CO₂ molecule are allowed to relax. The Brillouin zone integrations were performed in a grid of 3 × 3 × 1 k-points with the Monkhorst–Pack scheme.²² We use the nudged-elastic-band (NEB)²³ method to determine the minimum-energy paths for CO₂ adsorption, dissociation, and diffusion.

III. Results and Discussion

In our simulations, we note initially that only very weak molecular adsorption states with a small adsorption energy (E_{ads}

* To whom correspondence should be addressed.

[†] University College London.

[‡] Zhengzhou University.

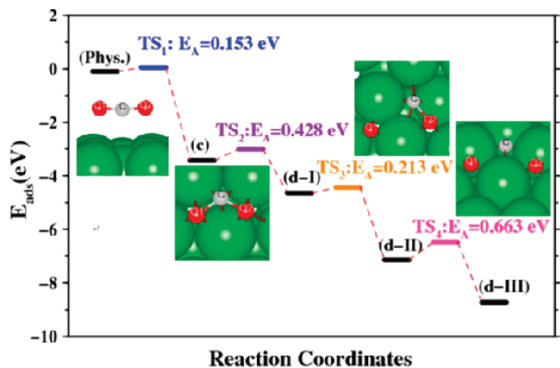


Figure 1. Reaction coordinates and four transition states (TS) for CO₂ molecule on Ti(0001) surface.

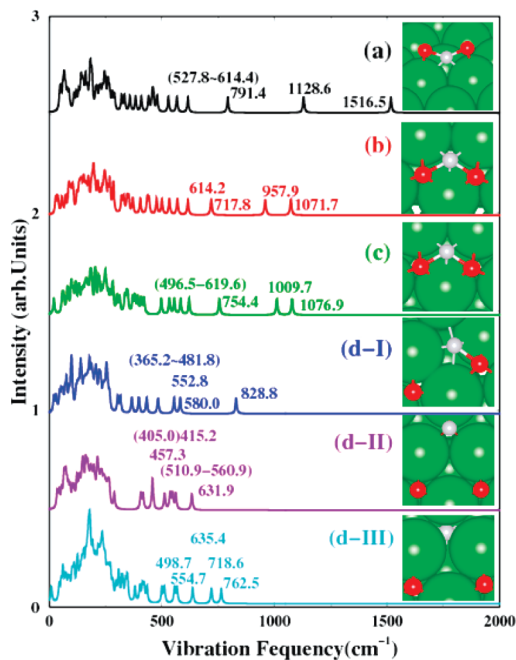


Figure 2. Structures and vibration frequency spectra for CO₂ adsorption on Ti(0001): (a), (b), and (c) represent chemisorption states of molecular CO₂; (d-I) and (d-II) dissociated configurations; and (d-III) a stable configuration with the C diffused into a sublayer. Ti atoms are in green, C in gray, and O in red.

$= E(\text{CO}_2/\text{Ti}(0001)) - E(\text{CO}_2) - E(\text{Ti}(0001)))$ of about -0.1 eV were obtained, if the initial distances between the mass center (MC) of the linear CO₂ molecule and the surface Ti atoms, $R(\text{MC-Ti})$, were set larger than ~ 3.2 Å followed by relaxation. However, we soon note that the CO₂ molecule can readily chemisorb on the Ti(0001) surface with a significantly bent structure by overcoming a small adsorption barrier of 0.153 eV (Figure 1). In the transition state, TS₁, the $R(\text{MC-Ti})$ is about 2.9 Å, and the CO₂ molecule is slightly curved with $\angle\text{O-C-O} = 172.632^\circ$ and $R(\text{C-O}) = 1.184$ Å. With all possible initial adsorption sites and various molecular orientations, three stable molecular chemisorption structures along with their vibrational spectra are obtained (Figure 2a–c). These spectra were derived from the eigenvalues of the dynamical Hessian matrix using the finite difference method. The spectra can be used as “fingerprint” for experimental identification of the adsorption states. Table 1 summarizes the geometrical data and the vibrational modes of the three molecularly chemisorbed CO₂ on the Ti(0001) surface. For comparison, the calculated and experimental structural data of free CO₂ are also given.

In Figure 2a, the CO₂ adsorbs on a short-bridge (S–B) site with the C close to the surface and the two O atoms pointing

TABLE 1: Structural Parameters, Vibrational Modes, and Adsorption Energies of CO₂ on Ti(0001)

CO ₂	$R(\text{C-O})$ (Å)	$\angle\text{O-C-O}$ (deg)	v_{as}	v_{s}	v_{b} (cm ^{−1})	E_{ads} (eV)
free CO ₂ , calc	1.177	180.0	2351.6	1296.8	625.7	
free CO ₂ , exp ^{1c}	1.171	180.0	2396.0	1351.0	672.0	
mode (a)	1.284	133.3	1516.5	1128.6	791.4	−2.125
mode (b)	1.393	115.8	1071.7	957.9	717.8	−3.320
mode (c)	1.386	115.2	1076.9	1009.7	754.4	−3.578

upward (C_{2v} symmetry, $\angle\text{O-C-O} = 133.313^\circ$), i.e., a bent configuration. The bond lengths are slightly extended, with $R(\text{C-O}) = 1.284$ Å and $R(\text{C-Ti}) = 2.100$ Å, respectively. The magnitude of E_{ads} (-2.125 eV, Table 1) is considerably greater than those of CO₂ on Co (-0.606 eV) and Ni (-0.240 eV) surfaces reported recently,^{12,13} though the adsorbed configurations are similar. The three high-frequency vibrational peaks (1516.5, 1128.6, and 791.4 cm^{−1}) in Figure 2a can be assigned to the CO₂ asymmetry stretching (v_{as}), symmetry stretching (v_{s}), and bending (v_{b}), respectively. The v_{as} and v_{s} modes are significantly red-shifted, compared with the calculated (2351.6 and 1296.8 cm^{−1}) and the experimental values (2396 and 1351 cm^{−1})^{1c} of a free CO₂ molecule, respectively; however, the v_{b} mode is clearly blue-shifted, from 625.7 to 791.4 cm^{−1}, due to the bending of the CO₂. This result further suggests that the CO₂ adsorbate is considerably activated on Ti(0001). In fact, Shea et al.¹² report that CO₂ favors a similar bridge site on the Co(110) surface, but it is weakly activated with relatively larger values of $v_{\text{as}} = 1906$, $v_{\text{s}} = 1245$, and $v_{\text{b}} = 617$ cm^{−1}. Another relatively stable chemisorption state yields an E_{ads} of -3.320 eV (Figure 2b), where the CO₂ molecule adsorbs horizontally on the Ti(0001) surface with $\angle\text{O-C-O} = 115.759^\circ$, and the C and O atoms occupy the surface face-centered cubic (SFCC) and the surface hexagonal close-packed (SHCP) hollow sites, respectively. The C–O bond length is further stretched to 1.393 Å, compared to that of the structure (a), due to enhanced interaction between the CO₂ adsorbate and the substrate. Consequently, the three high-frequency vibrational modes are red-shifted to 1071.7, 957.9, and 717.8 cm^{−1} (see Table 1).

The most stable molecular chemisorption state produces an E_{ads} of -3.578 eV, and the CO₂ configuration is similar to the structure (b), but with switched C and O adsorption sites and an adsorption angle of $\angle\text{O-C-O} = 115.190^\circ$ (Figure 2c). It seems surprising that the structure (c) possesses a slightly shorter bond length, $R(\text{C-O}) = 1.386$ Å, though its $|E_{\text{ads}}|$ is greater than that of structure (b) by 0.258 eV (Table 1). The main reason is because that an O(C) atom prefers the SFCC(SHCP) site to the SHCP(SFCC) site by $\sim 0.321(0.162)$ eV. Consequently, the characteristic vibrational modes of the structure (c) are $v_{\text{as}} = 1076.9$, $v_{\text{s}} = 1009.7$, and $v_{\text{b}} = 754.4$ cm^{−1}, which are all slightly larger than those of the structure (b), due to the shorter C–O bond length of the structure (c). This finding is helpful to avoid potential mistakes in experimental spectroscopic identification of the favorable molecular adsorption site based on the red shifts. It is also interesting to note that the most stable CO₂ structure on Ti(0001) is very different from those on Cu(110) (almost linear),¹⁴ Co(110) (S–B, C_{2v}),¹² and Ni(110) (on a 3-fold hollow-up site, where CO₂ occupies a hollow site on the surface and binds with three top-layer atoms).¹³

A modest activation energy ($E_{\text{A}} = 0.428$ eV, TS₂, Figure 1) is observed for CO₂ dissociation from the structures (c) to (d-I) with an energy gain of 1.291 eV. Here, we note that in structure (c) the two oxygen atoms occupy the SFCC site and in structure (d-I) the split CO species with bond length of 1.44 Å adsorbs almost flat on the surface. In the TS₂, $R(\text{C-O1})$ is activated to

1.40 Å and the $R(\text{C}-\text{O}_2)$ is 1.35 Å. On the right-hand side of the spectrum there is only one major high-frequency peak at 828.8 cm^{-1} due to the stretching mode of the CO moiety, which is much smaller than 2035.9 cm^{-1} for a free CO molecule (calculated), 1928 cm^{-1} for CO on Fe(110) (calculated),¹⁵ and 2064 cm^{-1} for CO on Cu(100) (experimental).²⁴ This red shift is a clear indication of significant activation of the CO moiety.

More intriguingly, the highly activated CO moiety can split further upon a weak perturbation of 0.213 eV (Figure 1, TS₃), sharply lowering the total energy by 2.477 eV (Figure 1(d-II)). The calculated E_{A} in TS₃ is significantly smaller than the calculated value of 1.52 eV for CO dissociation on Fe(110) surfaces.¹⁵ For TS₃, the carbon atom occupies the bridge site and the $R(\text{C}-\text{O}_2)$ is further activated to 1.69 Å, which is close to the value of 1.74 Å for CO dissociation on the Fe(110) surface.¹⁵ The separated C and O atoms adsorb in three neighboring SFCC sites at a distance $R(\text{C}-\text{Ti}) = 1.976$ and $R(\text{O}-\text{Ti}) = 1.947$ Å, respectively. The highest vibrational mode due to the stretching vibration between the C and the nearest-neighbor Ti atom in d-II is significantly red-shifted to 631.9 cm^{-1} . We further determined that the C split from the CO₂ adsorbate prefers to diffuse down to the OCT(1, 2) site (d-III) with an energy gain of 1.588 eV by overcoming a slightly larger activation barrier of 0.663 eV. Contrary to the previous cases, the high-frequency vibrational modes for the structure d-III are blue-shifted due to the enhanced C–Ti interactions. However, the oxygen atoms seem to favor the SFCC sites rather than the sublayer site of OCT(1, 2), Figure 2(d-III), which is in line with the adsorption behavior of O atoms on Ti(0001) reported previously.²⁵ The rather different C and O diffusion characteristics are due to the complex interplay of their sizes, Ti surface reconstruction, and the repulsive interactions of the O ions.

To clarify the continued activity of CO₂-adsorbed Ti(0001), we have also calculated the adsorption of a second CO₂ molecule on the structure d-III. Our results show that the second CO₂ also prefers a similar total dissociation state with that of the first one, from both the thermodynamic and kinetic points of view. Here, we also highlight that upon the diffusion of the second C atom a metastable structure is obtained with the formation of a tilted C–C dimer ($R(\text{C}-\text{C}) = 1.41$ Å), which may be the key step in the formation of organic structures with CO₂ as resources.

The mechanism for CO₂ adsorption on Ti(0001) is probed by analyzing the local projected density of state (DOS) and the electron charge density (CD) for the adsorption process of structure (c), with a starting $R(\text{MC}-\text{Ti}) = \sim 5.5$ Å (Figure 3). In the initial state, the oxygen states (Figure 3a2) localized about 5.0 eV below the Fermi level are the main contributor to the HOMO of the almost intact CO₂ molecule, as supported by the charge density (CD) analysis (Figure 3a). However, the LUMO of the intact adsorbate is mainly resulted from the carbon atom and locates far beyond the Fermi surface and invisible in the current energy range, Figure 3a1, which agrees well with the recent theoretical study for CO₂ on Co surfaces.¹² It is noted that in the range of -5.0 – 0.0 eV (E_{F}), there is no orbital mixing between the CO₂ and the Ti substrate (Figure 3a1–a3). Upon activation, in the TS₁, the CO₂ is slightly curved, introducing dipole moments and enhancing the attractive interaction between the activated CO₂ adsorbate and the Ti(0001) surface. Consequently, the CO₂ is readily bent and the LUMO is further lowered, which triggers a significant charge transfer from the Ti(0001) metal to the C and the O atoms of relatively large electron negativities. Meanwhile, the orbital mixing between the adsorbate and the d (s) electronic levels of the metal surface

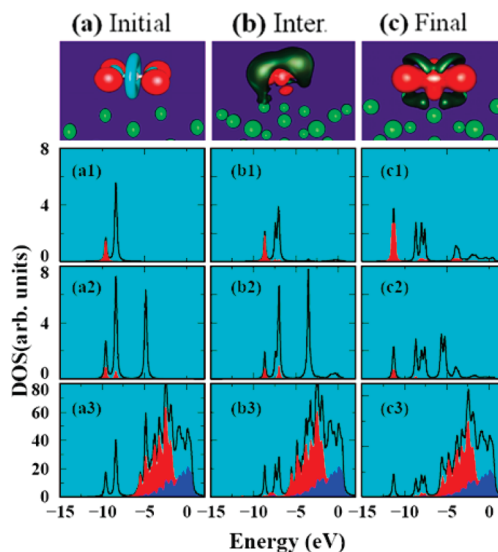


Figure 3. Total and partially projected DOSs (PDOSs) for the CO₂/Ti(0001) systems: (1) PDOSs for C; (2) PDOSs for O; and (3) total DOSs and PDOSs for Ti. The s-PDOS and d-PDOS are marked in red and blue, respectively. For the initial state, (a) the charge densities of the HOMO (in red) and the LUMO (in cyan) of the intact CO₂ molecule are presented. For the intermediate state (Inter.) (b) and the final chemisorption state (c) (the structure in Figure 1c), charge density differences are shown. Red: charge accumulation; green: charge depletion.

is also observed, as indicated by the DOS and the CD analysis for a randomly selected intermediate state (Figure 3b–b3), where the plane of the bent CO₂ is still perpendicular to the Ti(0001) surface with an angle of $\angle\text{O}-\text{C}-\text{O} = 139.583^\circ$ and the $R(\text{C}-\text{O})((\text{C}-\text{Ti})) = 1.21$ (2.75) Å. The activation of CO₂ molecule accompanied by charge transfer from metal substrate to the CO₂ moiety was also recently discovered in the cases of Fe,¹⁰ Co,¹² and Ni¹³ systems.

In the final chemisorbed state (Figure 3c–c3), the DOS projected on both the C and the O become complex due to the severely curved CO₂ structure and its interaction with the Ti surface. Importantly, for the carbon and the oxygen, new occupied peaks exist in the energy range of -5.0 – 0 eV (E_{F}), which are originated from the lowered LUMO of the activated CO₂ species. A Bader charge analysis²⁶ shows that ~ 1.4 electrons are transferred from the Ti atoms to the CO₂ species. Again, the orbital mixing between the p orbital of oxygen (carbon) atoms and the d levels of Ti(0001) is clearly observed by the Fermi surface, which enhances the binding between the adsorbate and the substrate. Consequently, the adsorbed CO₂ is significantly activated, and the strong Ti–C and Ti–O interactions render the dissociation of the CO₂ adsorbate. Here, we stress that for all the cases of adsorption, e.g., Figure 3c, the DOS by the Fermi surface is predominantly contributed by the Ti atoms, rather than the C and O atoms, implying that the vibrational frequency is a more fitting indicator than scanning tunneling microscopy (STM) for the analysis of CO₂ sorption states on the Ti(0001) surface, as supported by the Tersoff's tunnelling theory.²⁷

Finally, we note that for either O(C) atom or a CO₂ molecule the adsorption energy (E_{ads}) is correlated with the work function of a substrate. One can get that the E_{ads} is significantly large over Ti, among the early TM elements, and over Fe, Co, and Ni, among the late elements, upon screening of all the 3d TM elements, from Sc to Zn for the adsorptions of a single C and a single O atom (see Figure 4a) as well as of a CO₂ molecule.^{1b,12,13} The large adsorption energy of CO₂ on the early

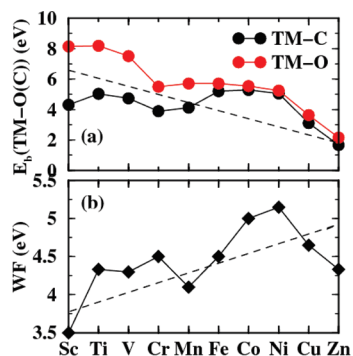


Figure 4. (a) Binding energy of C(O) atom with TM elemental atoms. (b) Work function of TM surfaces (cited from ref 28); dashed line: fitting data as a function of elements.

TM structures seems to be inversely proportional to their work functions²⁸ (see Figure 4b), in close agreement with the charge transfer mechanism; i.e., the smaller the work function of the early TM, the easier the charge transfer to the C/O atom (CO_2 species) (see the fitting lines in Figure 4a,b). Our findings also lend to the understanding of the experimental observation that Ti is significantly more effective than other light TM electrodes for electrochemical reduction of CO_2 .¹⁶ However, we also point that some late TM, such as Fe, Co, and Ni, can also significantly activate CO_2 with a large E_{ads} , though these elements possess relatively large work functions (Figure 4b); here the reason for the relatively strong activation of CO_2 on Fe, Co, and Ni is due to the charge transfer from the occupied antibonding states of these late TMs to C and O atoms of the adsorbed CO_2 species, reducing the electron–electron repulsive interactions involved in the antibonding states. This general phenomenon of correlation between adsorption energy for an adsorbate and the work function of the substrate is also supported by a recent systematic study on the adsorption of single TM atoms on a carbon nanotube²⁹ and the previous report on alkali promoted adsorption of CO_2 on Pt(111).^{11a}

Note also that for the very late transition metals, such as Cu and Zn, we observe a slightly contrast correlation between the adsorption energy and the work function, which can be due to the closed d electronic shell of Cu and Zn, implying some other higher order terms, such as hardness/softness as well as orbital hybridizations may also be considered to identify their chemical activity toward CO_2 , though the parameter of work function may be generally dominant.

IV. Summary

To summarize, we have identified that CO_2 molecules can be highly activated and totally reduced into elemental forms on the $p(3 \times 3)$ Ti(0001) surface as a result of significant charge transfer. Our findings reveal that the early TM elements such as titanium provide much stronger CO_2 activation than the late TMs studied so far due to their different electronic structures, such as smaller work functions, which is in good agreement with related experimental reports. It is also emphasized that the strong capability of Ti to activate CO_2 opens the possibility of designing suitable Ti_xTM_y alloys or other nanostructures of relatively small work functions for efficient catalysis and conversation of CO_2 . Further theoretical and experimental investigations are expected to follow this direction.

Acknowledgment. We thank Profs. Z. Y. Zhang and X. G. Gong and Drs. S. Meng and S. A. Shevlin for valuable discussions. This work was supported by the EPSRC under UK-SHEC (EP/E040071/1) and a Platform Grant (EP/E046193/1) (Z.X.G.) and the National Science Foundation of China under Grant No. 10604049 (S.F.L.).

References and Notes

- (1) (a) Freund, H.-J.; Messmer, R. P. *Surf. Sci.* **1986**, *172*, 1–30. (b) Freund, H.-J.; et al. *Surf. Sci.* **1987**, *180*, 550. (c) Freund, H.-J.; Roberts, M. W. *Surf. Sci. Rep.* **1996**, *25*, 225, and references therein.
- (2) (a) Yin, X.; Moss, J. R. *Coord. Chem. Rev.* **1999**, *181*, 27. (b) Stobrawe, A.; Makarczyk, P.; Maillet, C.; Muller, J.-L.; Leitner, W. *Angew. Chem., Int. Ed.* **2008**, *47*, 6674.
- (3) (a) Laitar, D. S.; Muller, P.; Sadighi, J. P. *J. Am. Chem. Soc.* **2005**, *127*, 17196. (b) Walton, K. S.; Millward, A. R.; Dubbeldam, D.; Frost, H.; Low, J. J.; Yaghi, O. M.; Snurr, R. Q. *J. Am. Chem. Soc.* **2008**, *130*, 406.
- (4) (a) Stampfl, C.; Scheffler, M. *Phys. Rev. Lett.* **1997**, *78*, 1500. (b) Rieger, M.; Rogal, J.; Reuter, K. *Phys. Rev. Lett.* **2008**, *100*, 016105.
- (5) Cudia, C. C.; Hla, S. W.; Comelli, G.; Šljivančanin, Ž.; Hammer, B.; Baraldi, A.; Prince, K. C.; Rosei, R. *Phys. Rev. Lett.* **2001**, *87*, 196104.
- (6) (a) Rogal, J.; Reuter, K.; Scheffler, M. *Phys. Rev. Lett.* **2007**, *98*, 046101. (b) Yamanaka, T.; Matsushima, T. *Phys. Rev. Lett.* **2008**, *100*, 026104.
- (7) Ackermann, M. D.; Pedersen, T. M.; Hendriksen, B. L. M.; Robach, O.; Bobaru, S. C.; Popa, I.; Quiros, C.; Kim, H.; Hammer, B.; Ferrer, S.; Frenken, J. W. M. *Phys. Rev. Lett.* **2005**, *95*, 255505.
- (8) Van Daelen, M. A.; Li, Y. S.; Newsam, J. M.; Van Santen, R. A. *J. Phys. Chem.* **1996**, *100*, 2279.
- (9) Hahn, J. R.; Ho, W. *Phys. Rev. Lett.* **2001**, *87*, 166102.
- (10) (a) Reddy, B. V.; Khanna, S. N. *Phys. Rev. Lett.* **2004**, *93*, 068301. (b) Jiang, D. E.; Carter, E. A. *Surf. Sci.* **2004**, *570*, 167. (c) Glezakou, V.-A.; Dang, L. X.; McGrail, B. P. *J. Phys. Chem. C* **2009**, *113*, 3691.
- (11) (a) Ricart, J. M.; Habas, M. P.; Clotet, A.; Curulla, D.; Illas, F. *Surf. Sci.* **2000**, *460*, 170. (b) Sremaniak, L. S.; Whitten, J. L. *Surf. Sci.* **2007**, *601*, 3755.
- (12) De la Peña O'Shea, V. A.; González, S.; Illas, F.; Fierro, J. L. G. *Chem. Phys. Lett.* **2008**, *454*, 262.
- (13) (a) Ding, X.; De Rogatis, L.; Vesselli, E.; Baraldi, A.; Comelli, G.; Rosei, R.; Savio, L.; Vattuone, L.; Rocca, M.; Fornasiero, P.; Ancilotto, F.; Baldereschi, A.; Peressi, M. *Phys. Rev. B* **2007**, *76*, 195425. (b) Wang, S.-G.; Gao, D. B.; Li, Y. W.; Wang, J. G.; Jiao, H. J. *J. Phys. Chem. B* **2005**, *109*, 18956. (c) Bartos, B.; Freund, H.-J.; Kuhlbeck, H.; Neumann, M.; Lindner, H.; Müller, K. *Surf. Sci.* **1987**, *179*, 59.
- (14) (a) Wang, G.-C.; Jiang, L.; Morikawa, Y.; Nakamura, J.; Cai, Z.-S.; Pan, Y.-M.; Zhao, X.-Z. *Surf. Sci.* **2004**, *570*, 205. (b) Funk, S.; Hokkanen, B.; Wang, J.; Burghaus, U.; Bozzolo, G.; Garcés, J. E. *Surf. Sci.* **2006**, *600*, 583.
- (15) Jiang, D. E.; Carter, E. A. *Surf. Sci.* **2004**, *570*, 167.
- (16) Azuma, M.; Hashimoto, K.; Hiramoto, M.; Watanabe, M.; Sakata, T. *J. Electrochem. Soc.* **1990**, *137*, 1772.
- (17) Khan, S. U. M.; Al-Shahry, M., Jr.; Ingler, W. *Science* **2002**, *297*, 2243.
- (18) Kresse, G.; Furthmüller, J. *Phys. Rev. B* **1996**, *54*, 11169. *Comput. Mater. Sci.* **1996**, *6*, 15.
- (19) Perdew, J. P.; Burke, K.; Ernzerhof, M. *Phys. Rev. Lett.* **1996**, *77*, 3865.
- (20) Kresse, G.; Joubert, D. *Phys. Rev. B* **1999**, *59*, 1758.
- (21) (a) Kittel, C. *Introduction to Solid State Physics*, 7th ed.; Wiley: New York, 1996. (b) Huda, M. N.; Kleinman, L. *Phys. Rev. B* **2005**, *71*, 241406(R).
- (22) Monkhorst, H. J.; Pack, J. D. *Phys. Rev. B* **1976**, *13*, 5188.
- (23) Henkelman, G.; Jónsson, H. *J. Chem. Phys.* **2000**, *113*, 9978.
- (24) Tracy, J. C. *J. Chem. Phys.* **1972**, *56*, 2748.
- (25) Liu, S. Y.; Wang, F. H.; Zhou, Y. S.; Shang, J. X. *J. Phys.: Condens. Matter* **2007**, *19*, 226004.
- (26) Henkelman, G.; Arnaldsson, A.; Jónsson, H. *Comput. Mater. Sci.* **2006**, *36*, 354.
- (27) Tersoff, J.; Hamann, D. R. *Phys. Rev. B* **1985**, *31*, 805.
- (28) Michaelson, H. B. *J. Appl. Phys.* **1977**, *48*, 4729.
- (29) Durgun, E.; Dag, S.; Bagci, V. M. K.; Gülseren, O.; Yildirim, T.; Ciraci, S. *Phys. Rev. B* **2003**, *67*, 201401(R).